ISSN 1062-8738, Bulletin of the Russian Academy of Sciences: Physics, 2023, Vol. 87, No. 5, pp. 552–558. © Allerton Press, Inc., 2023.
Russian Text © The Author(s), 2023, published in Izvestiya Rossiiskoi Akademii Nauk, Seriya Fizicheskaya, 2023, Vol. 87, No. 5, pp. 627–634.

Superconducting Undulator with a Period of 15.6 mm and Magnetic Field of 1.2 T

V. A. Shkaruba[a, b, *], A. V. Bragin[a], A. A. Volkov[a, b], A. I. Erokhin[a], A. V. Zorin[a], F. P. Kazantsev[a], P. V. Kanonik[a], N. A. Mezentsev[a, b], A. N. Safronov[a], A. A. Sedov[a], O. A. Tarasenko[a], S. V. Khrushchev[a, b], and V. M. Tsukanov[a, b]

[a] *Budker Institute of Nuclear Physics, Siberian Branch, Russian Academy of Sciences, Novosibirsk, 630090 Russia*
[b] *SKIF Synchrotron Radiation Facility, Boreskov Institute of Catalysis, Siberian Branch, Russian Academy of Sciences, Koltsovo, 630559 Russia*
**e-mail: shkaruba@mail.ru*

Received November 28, 2022; revised December 15, 2022; accepted January 25, 2023

Abstract—A superconducting undulator created at the Budker Institute of Nuclear Physics with a period of 15.6 mm and a field of 1.2 T is tested in own undulator cryostat based on indirect cooling with zero helium consumption. The main characteristics and design features of the magnetic and cryogenic systems of this insertion device are presented. Results from measuring the magnetic field are presented. Features of the operation of a cryogenic system in different modes are discussed.

DOI: 10.3103/S1062873822701830

INTRODUCTION

Superconducting undulators are the most demanded devices for generating synchrotron radiation (SR) using modern SR sources. Superconducting technologies offer the highest magnetic field level with a minimum period, in comparison to similar devices based on permanent magnets [1–3]. These technologies enable SR sources with energies up to 3 GeV to yield radiation with spectral characteristics not inferior in brightness and magnitude of the photon flux to machines with higher energy. A superconducting undulator with a period of 15.6 mm and a field of 1.2 T was created at the Budker Institute of Nuclear Physics and examined in own undulator cryostat based on indirect cooling with zero helium consumption. The magnetic structure of the undulator is based on alternating active and neutral poles [4, 5]. The phase error was calculated from measurements of the magnetic field and does not exceed 3°, which is a necessary condition for the undulator to work. The main parameters of the undulator are presented in Table 1.

MAGNETIC SYSTEM OF THE UNDULATOR

The magnetic system of the undulator, which creates a vertical magnetic field with periodically changing polarity, consists structurally of upper and lower halves and is based on alternating active and neutral poles. Such a scheme was obtained by transformation from a conventional magnetic structure, where all poles consist of windings of the horizontal racetrack type, wound around an iron core, and located opposite each other. In the straight sections of such a structure, the currents in adjacent windings flow co-directionally. These sections were combined into single windings of double thickness and closed alternately from the outside in one direction or the other. The magnetic field of all active poles on each of the halves of the magnet is directed towards each other, and both

Table 1. Main parameters of the undulator

Parameter	Value
Nominal magnetic field, T	1.2
Wiggler period, mm	15.6
Interpolar gap, mm	8
Vertical aperture for beam, mm	6
Horizontal aperture for beam, mm	60
Number of periods	119
Magnetic length, mm	~1900
Length between flanges	~2500
Winding current, A	~500
Radiation power (at $B = 1.2$ T, $I = 0.4$ A, $E = 3$ GeV), kW	~7
Horizontal radiation angle, mrad	±0.32
RMS phase error, deg	<3
Maximum value of deviation parameter K	~1.73

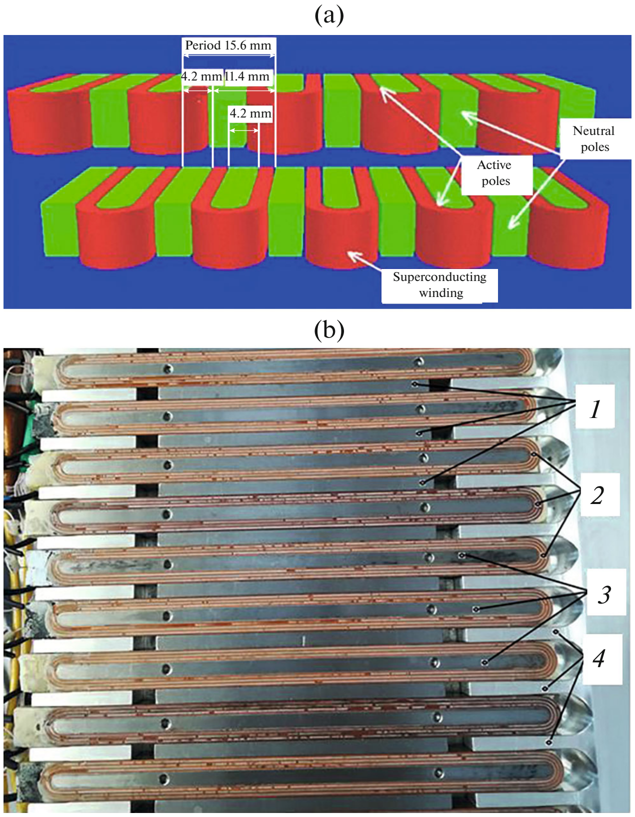

Fig. 1. Magnetic structure of the undulator with alternating active and neutral poles: (a) 3D model and (b) appearance.

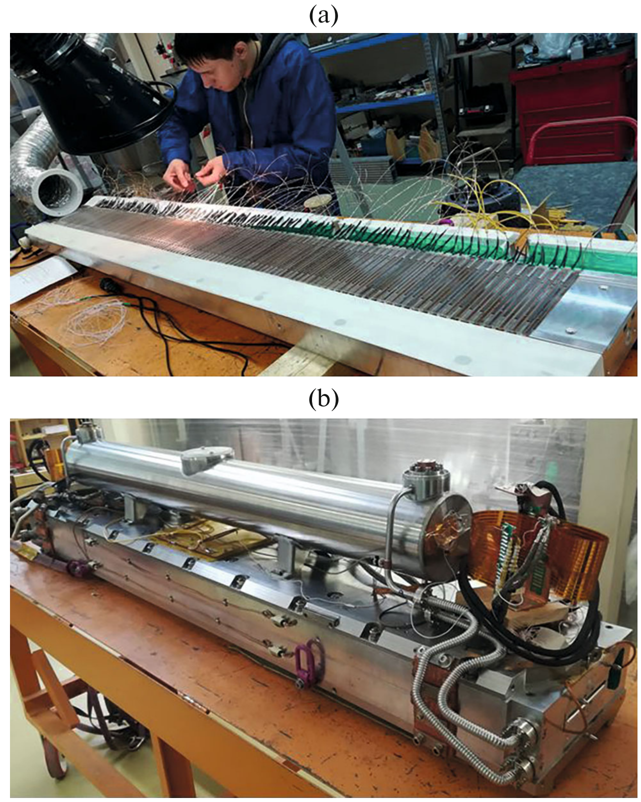

Fig. 2. Appearance of the undulator magnet: (a) halves of the magnet in the process of assembly and (b) the magnet assembled with the helium vessel installed.

halves are shifted relative to each other by half a period. Each active pole with its own winding and positioned on one half of the magnet, is thus opposite a neutral pole of the other half, as shown in the 3D model in Fig. 1a. The period value of 15.6 mm is the sum of the width of one active pole with a size of 11.4 mm and one neutral pole with a width of 4.2 mm. Figure 1b shows the appearance of the finished magnetic structure with alternating active and neutral poles.

The main element of the magnetic structure is a superconducting coil wound around an iron core. The design of the coil has been optimized to obtain the maximum field in the beam orbit. Inside the interpolar gap 8 mm high, there is a vacuum beam chamber with a wall thickness of 0.5 mm at a distance of 0.5 mm. The vertical aperture of the vacuum chamber for the electron beam is thus 6 mm in size. We used a superconducting Nb–Ti/Cu wire with a diameter of 0.55 mm, including varnish insulation, that had a critical current of 260 A in a field of 7 T. The optimum staggered winding consists of 7 layers and 12 turns in each full layer. The maximum field in the critical region of the winding at a current of 500 A is 4.25 T, which corresponds to a field level of 1.2 T on the undulator axis.

The magnetic structure of the undulator consists of 119 main periods with a nominal magnetic field of 1.2 T in the orbit and side coils with a field of 3/4 and 1/4 of the main field, which serve to nullify the field integrals and close the beam orbit. To protect the windings in the event of lost of superconductivity, chains of series-connected diodes and resistors connected in parallel to the main windings were used. Figures 2a and 2b show the appearance of half of the magnet in the assembly process and the appearance of the undulator magnet in collection, respectively.

A circuit with neutral and active poles allows us to halve the number of coils in the undulator. The number of electrical contacts between the coils is also halved, and the power released at these connections during the flow of current is thus reduced. Another advantage of this circuit is that the action of ponderomotive forces that push two adjacent windings apart in a magnet of the usual configuration is balanced in this scheme, since the forces are directed inside the combined double-thickness winding. Superconducting windings thus become more resistant to the loss of superconductivity, due to the limited movement of the coils of wire under the action of ponderomotive forces. This enables the coils to fit into the magnet slots without using the special mechanical banding required in conventional design. The upper and lower halves of the magnet are made of 6063 aluminum alloy, which has high thermal conductivity in the operating temperature range of ~3 K. This is essential for a dry magnet with indirect cooling, operating in a vacuum. Structurally, this scheme ensures high accuracy with a stable period size over the entire length of the undulator, minimizing the contribution of the period length error to the phase error.

CRYOGENIC UNDULATOR SYSTEM

The cryogenic system of an undulator with zero helium consumption operates by the principle of indirect cooling. The magnet is inside a vacuum rather than a vessel with liquid helium, and all elements of the cryostat are cooled by cryocoolers [6]. This allows us to remove the chamber of the helium vessel from the magnetic gap and use only one vacuum chamber to pass the beam and raise the level of the magnetic field by reducing the magnitude of the magnetic gap.

The principle of operation of a cryostat with zero helium consumption is based on the interception of all heat inflows from the outside of the cryostat, along with the heat released inside the cryostat from the flowing current and the effect of the electron beam, on the corresponding stages of the cryocoolers. The cryostat uses two Sumitomo SRDK-415D cryocoolers and two Sumitomo SRDK-408S cryocoolers. The operating temperature of the magnet is maintained at ~3.5 K by the circulation of liquid helium through channels drilled in the upper and lower halves of the magnet. Liquid helium is in a small 30-L vessel, located outside the magnet in the protective vacuum of the cryostat. The evaporated helium is cooled and recondened by two second stages of SRDK-415D cryocoolers with a power of 1.5 W, at a temperature of 4.2 K through copper heat exchangers built into a helium vessel.

Current is fed into the magnet windings through combined current leads consisting of brass rods connected with one another in series and ceramic HTSC current leads, cooled by the corresponding stages of SRDK-415D cryocoolers. The influx of heat coming from the outside through the optimized brass current lead, along with the Joule heat released during the flow of current, is intercepted at the point of contact with the internal HTSC current lead by the first stage of the cryocooler with a temperature of 60 K. The lower part of the internal HTSC current lead is cooled by a 4 K cryocooler stage. The copper thermal screen of the cryostat is cooled simultaneously by all four 60 K stages of cryocoolers with a total cooling power of 180 W. Figure 3a demonstrates the design of a cryostat based on indirect cooling.

The beam chamber, extruded from 6063 aluminum alloy, has walls 0.5 mm thick. It is positioned with a gap of 0.5 mm from the surface of the superconducting poles. The internal aperture of the vacuum chamber is 6 mm vertically and 60 mm horizontally. Additional copper heat conductors are used to increase the efficiency of removal of heat induced in the chamber walls by image currents and synchrotron radiation, cooled by the second stages of the lower SRDK-408S cryocoolers with a minimum temperature of 8 K. The cross section of the magnetic gap with a vacuum chamber inside is shown in Fig. 3b.

The cooling power of the first stages of SRDK-415D cryocoolers with a temperature of 60 K is used to precool the magnet to operating temperatures. Two siphon-type nitrogen heat pipes are used as heat conductors, connecting the stages of the cryocooler with the magnet, each of which removes heat with a power of up to 100 W [7]. The thermal connection between the magnet and the cryocooler is automatically interrupted when the freezing temperature of nitrogen reaches ~64 K. Resistive heaters, controlled by a special algorithm based on measuring the temperature of nitrogen, are used to prevent premature freezing of heat pipes and increase their efficiency. Upon reaching the minimum possible temperature with the help of heat pipes, further cooling of the magnet is due only to the circulation of helium, cooled by the second stages of SRDK-415D cryocoolers through copper heat exchangers in the helium vessel.

A feature of the operation of this cryostat is the complete elimination of liquid refrigerants during both cooling down and long-term operation. Only gaseous helium fed into the vessel directly from a compressed cylinder, is used for precooling and reaching the operating temperature. When gaseous helium is supplied from a cylinder, constant absolute pressure is maintained at a level of ~1.8 bar using a reducing gear. The cryostat is equipped with an emergency pressure relief valve that operates at a pressure of ~2 bar in the vessel. The density of the helium in the cryostat gradually rises as the temperature falls. Helium liquefaction begins upon reaching the appropriate temperature, and its level in the helium vessel increases. Just one standard cylinder with gaseous helium containing ~5.7 m^3 of gas, which is equivalent to ~8 L of liquid helium, is sufficient to cool the magnet to operating temperature and reach a helium level of ~10%.

The total calculated heat influx into the cryostat for the cold mass with a temperature of 4.2 K is ~2 W, and the corresponding total cooling power of the second stages of the SRDK-415D cryocoolers is ~3 W. An excess cooling power of ~1 W in the thermal balance of the cryostat therefore results in supercooling of the magnet to a temperature of ~3.5 K and a corresponding drop in the absolute pressure in the helium vessel cut off from the outer atmosphere to ~0.7 bar. The cryostat thus does not consume liquid helium, and it operates at a pressure below that of the external atmosphere. Not only does operating at low temperatures increase the reliability of the cryostat and extend the service life of cryocoolers by reducing the thermal

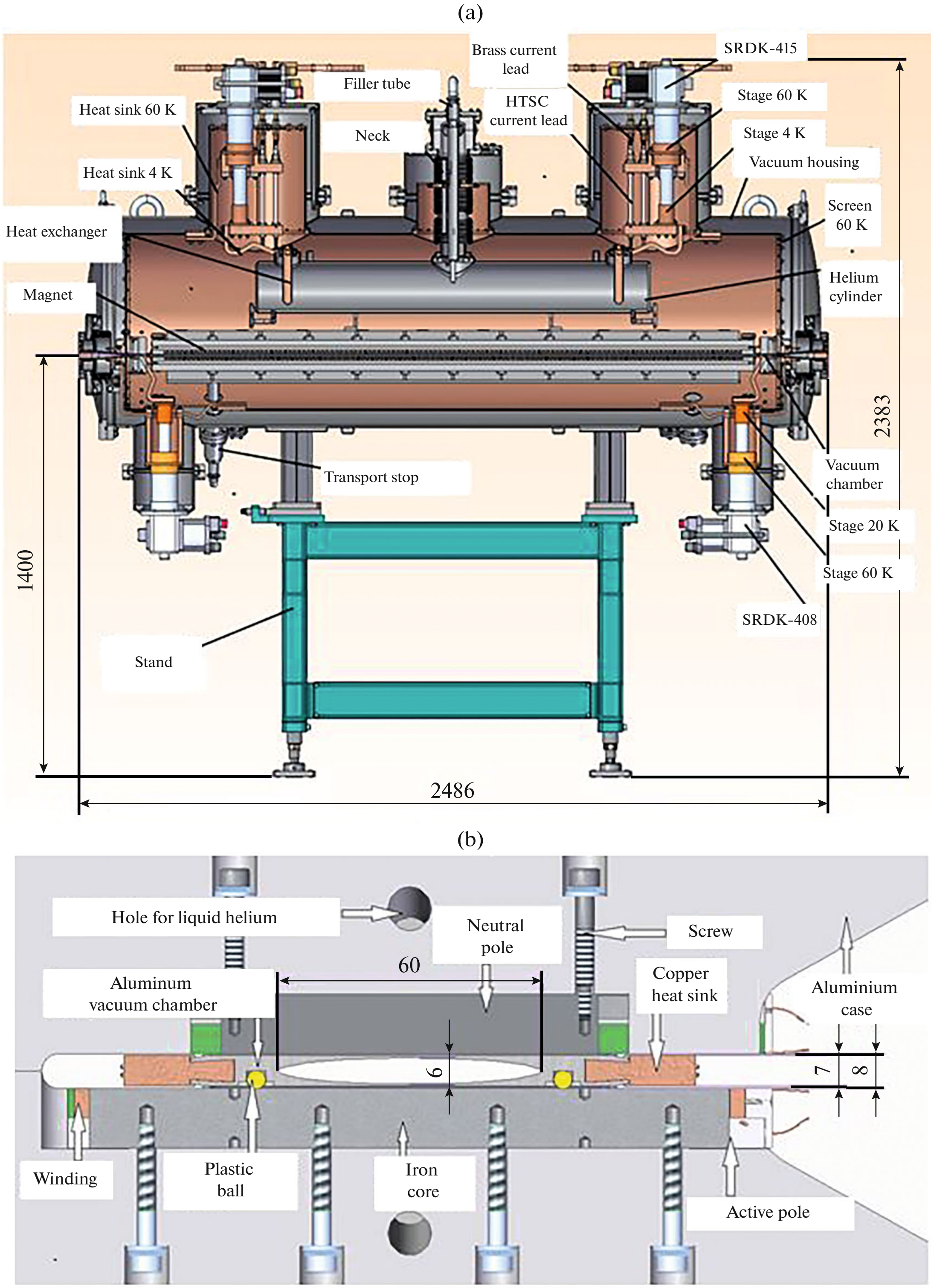

Fig. 3. Design of the undulator cryostat based on indirect cooling: (a) longitudinal section of the cryostat and (b) section of the magnetic gap with a vacuum chamber inside.

load, it also makes allows us to raise the level of the magnetic field due to a shift in the current characteristic of the superconducting wire. Negative pressure also creates an additional buffer volume in the helium vessel that allows us to keep the volume of helium in the cryostat constant during the breakdown of superconductivity, since the pressure in the vessel does not exceed the emergency valve actuation pressure of

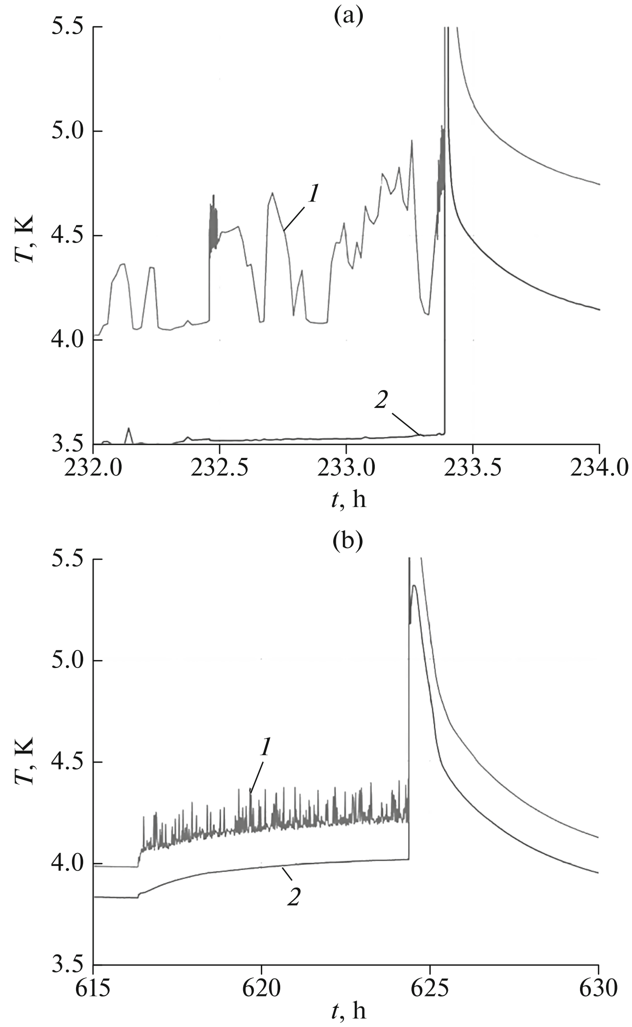

Fig. 4. Change in the temperature of (1) the Nb–Ti contact and (2) magnet: (a) raising the contact temperature to 5 K without additional cooling and (b) stabilizing the temperature at 4.3 K with additional cooling.

~2 bar. In this mode, the cryogenic system of the undulator allows us to operate autonomously inside the bioshield of the synchrotron for several years.

TEST RESULTS

In manufacturing the undulator, we performed several cycles of testing a full-sized 119-period undulator in own undulator cryostat with indirect cooling. One feature of magnetic field measurements in such an undulator is that with such a small "cold" interpolar gap of 8 mm, the corresponding vertical aperture of the vacuum chamber for the beam, which is only 6 mm, does not allow us to placing a measuring chamber with a "warm" aperture in it. It is sufficient to install a measuring carriage with a Hall sensor. Our own chamber was therefore replaced with a specially made aluminum measuring chamber that had an accessible vertical aperture of 5.5 mm open to the atmosphere, in order to make magnetic measurements. A thermal screen made of copper foil 0.2 mm thick with a temperature of ~20 K and several layers of screen-vacuum insulation with nylon spacers were placed in the accessible gap between the superconducting windings and the external atmosphere (0.75 mm) in order to insulate the measuring chamber. Despite thermal insulation, the temperature inside the warm gap of the measuring chamber did not rise above 50 K, which created additional difficulties for magnetic measurements with the Hall sensor and required additional correction of the measurements, allowing for the true temperature.

To exclude uncontrolled heating of the superconducting windings of the undulator from the side of the measuring chamber, the undulator with an evacuated gap between the magnet poles was first switched on with no chamber at all. During training, the field was raised rapidly for 5 min at a rate of ~2 A/s, and the maximum field level of 1.26 T was reached. However, the field level ensuring long-term stable operation did not exceed 1.15 T. At higher fields, there was an uncontrolled loss of superconductivity several minutes after the field was set. The effect of temperature pulsation on the contacts between series-connected windings was discovered when a certain threshold current was exceeded. When the current reached more than ~250 A, the contact temperature thus grew gradually from 4 K and began to pulsate with a period of ~2–4 s with amplitudes up to 5 K. A further slow increase in current led to a general heating of the magnet and a breakdown of superconductivity. Since the residual resistance of contacts between windings fabricated by cold welding of superconducting wires did not exceed $\sim 10^{-10}\ \Omega$, the release of Joule heat at a current of 500 A should not have exceed ~10 mW. However, the observed effect of temperature pulsation could lead to additional controlled heating. To eliminate the detected effect, which is probably due to jumps in the magnetic flux inside the joints of superconducting wires, each of the ~240 contacts was additionally cooled by electrically insulated copper heat conductors that remove heat directly to the magnet body. The next test of the undulator, performed with the measuring chamber already installed, showed that although the temperature pulsations persisted, the temperature at the contact fell to 4.3 K, ensuring stable operation in the 1.22 T field for several days. The behavior of the contact temperature before and after additional cooling is shown in Figs. 4a and 4b, respectively. The schedule for training the magnet to obtain the maximum magnetic field is shown in Fig. 5. The voltages arising on the undulator windings during breakdowns of superconductivity with a duration of no more than 10 ms did not exceed safe 150 V.

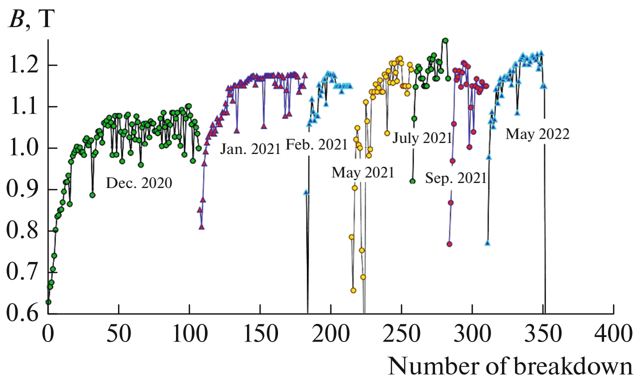

Fig. 5. Chart for training the undulator magnet to obtain the strongest possible magnetic field.

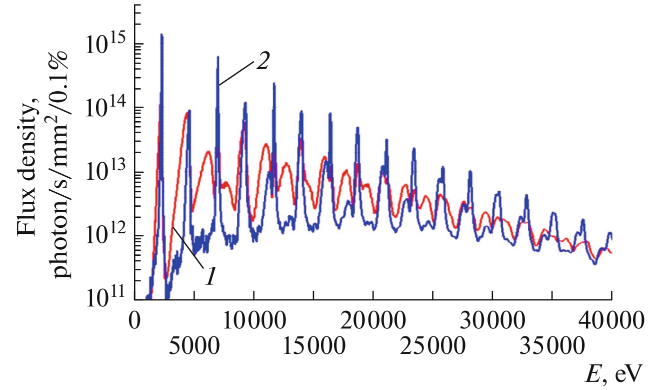

Fig. 6. Emission spectra calculated with the SPECTRA program based on (*1*) uncorrected and (*2*) corrected magnetic fields of the undulator ($E = 3$ GeV, $I = 400$ mA, $\varepsilon_x = 75$ pm rad, $B = 1.2$ T).

PHASE ERROR

The criterion for the quality of an undulator is the magnitude of the phase error, which characterizes the difference between the magnetic field of a real device and an ideal sinusoidal field, which should be only 3°. When using undulators to generate radiation in modern SR sources with small emittance and energy spread, the value of this parameter especially increases, since a large phase error limits the radiation brightness at high harmonics and does not allow full use of the storage ring capabilities.

The quality of the magnetic field of the undulator determines the magnitude of the phase error, which grows with an increase in the difference in the field amplitude between the poles, along with a change in the period along the length of the undulator. The difference in the field amplitude increases not only with a change in the magnetic gap but also with a spread in the geometric dimensions of the windings, as well as inaccuracies in the installation of the windings in the magnet frame. According to estimates, these differences should not exceed 10–20 μm. Inaccuracies in the period size were minimized along the length of the magnet, since the slots for installing the coils were milled to precisely this accuracy. However, we cannot ensure the same repeatability in the manufacture of the superconducting poles themselves. The magnitude of the phase error of the undulator, calculated from magnetic measurements by the Hall sensor immediately after manufacturing the undulator, was therefore more than 5°.

To lower the phase error, several successive permutations of the poles were made on the basis of measurements of the magnetic field amplitudes. The purpose of the first permutation was to obtain a smooth change in the magnetic gap along the entire magnet. Local permutations of the poles were then made with field amplitudes very different from one another. However, the strong mutual influence of the magnetic field of neighboring coils prevents the accurate determination of the field amplitude at each pole, so the phase error could not be reduced to less than 4°. Further attempts to improve the quality of the magnetic field by local changes in the magnetic structure did not produce a notable drop in the phase error, so we proposed a new means of correction.

Since the errors in the field amplitudes between the poles did not exceed ~1%, all series-connected windings on each of the halves of the magnet were divided into 12 identical sections, each of which was powered by a separate corrective current source up to 5 A, which is ~1% of the maximum operating current of 500 A. Using the ability to change the currents in each group of coils independently, we proposed the following phase error correction algorithm: In a structure with active and neutral poles, the magnetic field on all poles of the upper half of the magnet is directed downwards, toward the axis of the undulator, and upward on the lower half. It therefore becomes possible to change the field value equally at all poles of each of the correction sections independently. In the first stage, corrective magnetic fields were simultaneously created in each of the two sections of the upper and lower halves located opposite to each other; the corrective fields were either co-directional or opposite to the main direction of the field in each of these sections. This minimized the difference in magnetic field levels between all 12 corrected areas. At the next stage, the correcting fields in opposite sections were created already co-directed with each other, either downward or upward, which yielded additional dipole fields on the undulator axis, locally correcting the beam orbit in each of the 12 sections. Corrective currents whose superpositioning allowed us to correct the level of the magnetic field and the beam orbit in the undulator at each of these two stages simultaneously, were thus selected. The correction of the value of the integral phase error calculated from the corrected magnetic field distribution along the undulator was 2.9°, and the local phase error dropped to 1.9°. Figure 6 shows the

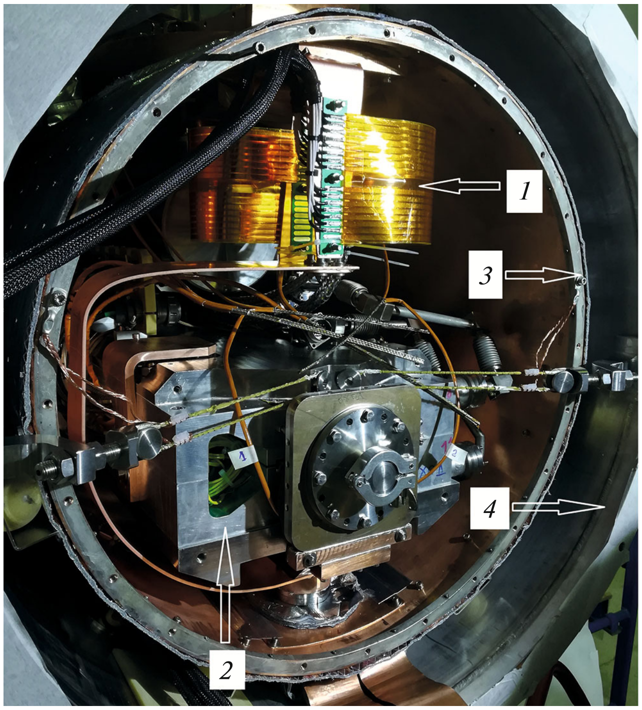

Fig. 7. Design of combined current leads for input of phase error correction currents: (*1*) current leads, (*2*) magnet, (*3*) shield, and (*4*) cryostat case.

emission spectra calculated by the SPECTRA program [8] based on the uncorrected and corrected magnetic fields of the undulator for an electron beam energy of 3 GeV, a current of 0.4 A, and an emittance of 75 pm rad; i.e., the spectral emission peaks after the correction of the magnetic field increased significantly for all harmonics.

The undulator windings were powered by corrective currents through special combined current leads consisting of a series-connected copper wire optimized for current flow up to ~5 A, an HTSC tape, and Nb–Ti wire. The junctions of all sections of the combined current leads were cooled to one another through isolated heat intercepts by the corresponding stages of cryocoolers with temperatures of 60, 20, and 4 K. The appearance of the combined current leads for introducing phase error correction currents is shown in Fig. 7.

CONCLUSIONS

A full-size 119-pole superconducting undulator with a period of 15.6 mm, a magnetic field level of 1.2 T, and a beam aperture of 6 mm was successfully tested in own undulator cryostat based on indirect cooling. A stable long-term magnetic field level of over 1.2 T was obtained during the tests. We proposed and applied a means of correction that yielded a phase error of less than 3°. Reliable long-term operation of a cryogenic system with indirect cooling was also demonstrated, allowing us to operate autonomously inside the bioprotection of the storage ring for several years.

FUNDING

This work was performed as part of a State Task for the Institute of Solid State Chemistry and Mechanochemistry from the RF Ministry of Science and Higher Education, agreement no. 075-15-2021-1359 and project no. FWUS-2021-0004.

CONFLICT OF INTEREST

The authors declare that they have no conflicts of interest.

REFERENCES

1. Gluskin, E. and Mezentsev, N., in *Synchrotron Light Sources and Free-Electron Lasers*, Jaeschke, E., Khan, S., Schneider, J., and Hastings, J. Eds., Cham: Springer, 2020, p. 935.
2. Kasa, M., Borland, M., Emery, L., et al., *Phys. Rev. Accel. Beams*, 2020, vol. 23, no. 5, p. 050701.
3. Casalbuoni, S., Blomley, E., Glamann, N., et al., *AIP Conf. Proc.*, 2016, vol. 1741, p. 020002.
4. Mezentsev, N.A., Khruschev, S.V., Shkaruba, V.A., et al., *Proc. Russ. Particle Accelerator Conference RuPAC2016*, St. Petersburg, 2016, p. TUCAMH01.
5. Bragin, A., Khrushchev, S., Lev, V., et al., *IEEE Trans. Appl. Supercond.*, 2018, vol. 28, no. 4, p. 4101904.
6. Bragin, A., Gusev, Ye., Khrushchev, S., et al., *Phys. Procedia*, 2016, vol. 84, p. 54.
7. Tsukanov, V.M., Khrushchev, S.V., Mezentsev, N.A., et al., *AIP Conf. Proc.*, 2020, vol. 2299, p. 020018.
8. Tanaka, T. and Kitamura, H., J. *Synchrotron Radiat.*, 2001, vol. 8, no. 6, p. 1221.

Translated by O. Zhukova